Sensors and Materials, Vol. 31, No. 2 (2019) 531–542
MYU Tokyo

S & M 1793

Mechanical Properties of Cobalt-based Alloy Coating Applied Using High-velocity Oxygen Gas and Liquid Fuel Spraying Processes

Cheng-Fu Yang,[1] Wei-Lung Pai,[2] Chao-Ming Hsu,[2*] and Cheng-Yi Chen[3**]

[1]Department of Chemical and Materials Engineering, National University of Kaohsiung, Kaohsiung 811, Taiwan
[2]Department of Mechanical Engineering, National Kaohsiung University of Science and Technology, Kaohsiung 80778, Taiwan
[3]Department of Electrical Engineering/Super Micro Mass Research and Technology Center, Cheng Shiu University, Kaohsiung 83347, Taiwan

(Received October 15, 2018; accepted December 13, 2018)

Keywords: high-velocity oxygen gas fuel, high-velocity oxygen liquid fuel, thermal spray, cobalt-based alloy, Inconel 718 nickel alloy

High-velocity flame thermal spraying technology is widely used to apply coatings on industrial and aerospace parts, because a high flame speed yields coatings with high bonding force, high density, and low porosity. In this study, high-velocity oxygen gas fuel (HVOGF) and high-velocity oxygen liquid fuel (HVOLF) spraying processes were used to spray commercial powders of cobalt-based materials onto Inconel 718 substrates, and the flame characteristics of the two processes were observed using a real-time monitoring system during the spraying process. The metallographic and mechanical differences between the coatings produced by these two heat sources were then analyzed. The results showed that the velocity of particles produced with HVOLF was 1.23 times higher than that with HVOGF. Consequently, the melted powder produced with HVOLF led to a more compact metallographic structure. The resulting average values of microhardness and bonding strength were, respectively, 1.20 and 1.65 times higher with HVOLF than with HVOGF.

1. Introduction

In the design of mechanical components, material selection is based on the mechanical strength of a given part when it is required to withstand a load. Selection should also take into account factors arising from the environment in which the part is used, such as corrosion, wear, and temperature, to maintain the part's capacity to function during duty cycles. When environmental conditions cannot be factored in material selection, coating techniques can provide additional layers of materials that resist environmental effects or that impart special functionality to the part's surface. Coatings can enhance the part's performance by providing multifaceted protection features, such as wear resistance, high-temperature resistance, corrosion

*Corresponding author: e-mail: jammy@kuas.edu.tw
**Corresponding author: e-mail: k0464@gcloud.csu.edu.tw
https://doi.org/10.18494/SAM.2019.2166

resistance, and heat insulation. A wide variety of surface-modification technologies, including electroplating, physical vapor deposition (PVD), chemical vapor deposition (CVD), and thermal spraying, are used.

A material applied to the surface of a given part is generally referred to as a coating or a film.[1,2] The thickness of coatings applied by PVD and CVD in aircraft industry applications is usually between 1 and 50 μm. Thermal spraying technology forms significantly thicker coatings with thicknesses of about 50 μm to 5 mm.[3,4] Thermal spraying deposits a coating onto a substrate by heating a powder of metal, ceramic, or cermet to a temperature close to or above its melting point, in order to improve the substrate surface properties. Such coatings can be used to repair parts and extend their service life. Thermal spraying is characterized by large spray areas, high speed, good stacking efficiency, and low thermal stress. Parts do not experience distortion or deformation problems before or after thermal spraying because the temperature is about 150 °C. A wide range of functional materials are available, and the coatings produced can be used in environments characterized by high-temperature oxidation, corrosion, and abrasion, highlighting the benefits of this technology.[5–7]

Hard chrome plating is a simple, low-cost process commonly used to form a protective layer on a substrate surface to resist corrosion and wear. However, this process entails serious environmental and health hazards caused by the generation of hexavalent chromium wastewater. Hence, new materials and coating techniques must be developed to overcome these shortcomings without compromising performance. High-velocity oxygen fuel (HVOF) spraying is a coating process that uses high-speed jet technology with heated powder to prepare a coating with very low porosity and high bonding force. Compared with atmospheric plasma spraying, the molten powder particles in HVOF are faster, have higher momentum and lower temperature, and do not evaporate when they hit the substrate, so the HVOF spraying process is suitable for achieving superhard alloy coatings.[8–12] This deposition process has little environmental impact and is regarded as the most promising substitute for hard chrome plating; indeed, the US Federal Aviation Administration has approved this process for spraying many parts of aircraft engines.[13]

The temperature generated by HVOF spraying can reach 2000–3000 °C. When no powder has been added, the airflow speed can be 4.5–6 times the speed of sound; with powder, it is 1–3 times the speed of sound. At such a speed, molten particles have no time to react with oxygen or gas; hence, there is very little production of oxides that otherwise might affect the coating's properties. When particles hit the substrate surface, a very high regional pressure is generated, causing local molten particle softening and forming a very thin diffusion coating, since the particles' kinetic energy is further converted into heat energy. The coating's internal layer structure is therefore dense and the bonding force is about 48.26–82.74 Mpa. The high density and low porosity achieved by HVOF spraying are conducive to repairing parts, and this process yields better results than other spraying processes.[14–16] Song *et al.*[17] studied Ni50Cr coatings formed using high-velocity oxygen gas fuel (HVOGF) and high-velocity oxygen liquid fuel (HVOLF) spraying processes, examining their microstructure and high-temperature oxidation by X-ray and X-ray diffraction analyses. Fiedler *et al.*[18] used HVOLF technology to spray metallic coatings on complex mechanisms and analyzed their temperature-dependent

mechanical properties using finite element simulation and experimental results. Puddu *et al.*[19] used HVOLF technology to achieve suspension spraying of TiO_2 coatings and analyzed their microstructural and tribological characteristics.

The purpose of this study is to use HVOGF and HVOLF techniques to spray a commercial powder of cobalt-based alloy material onto a substrate surface (test pieces) and then compare the mechanical properties of the test pieces in order to understand the differences between the techniques and how to correctly apply them. In a spraying process, a high-sensitivity sensor is used to analyze the particle velocity, torch temperature, and flame flow intensity generated by the two heat sources. The sprayed test pieces are analyzed using an optical microscope to examine unmelted particles and pores in the coating. In addition, a hardness test, a microhardness test, and a bonding force experiment are conducted to explore the differences between the mechanical properties of the coatings made using the two heat sources. The results indicate how the two spraying processes can be used effectively to achieve the desired performance by applying coatings on parts.

The remainder of this paper is structured as follows. In Sect. 2, the experimental method is described. In Sect. 3, the experimental results are presented and discussed. Finally, in Sect. 4, the conclusions drawn from the experimental and simulation results are presented and future work is described.

2. Experimental Methods

HVOGF and HVOLF technologies are used to spray cobalt-based Co–Mo–Cr–Si alloy powder onto the surface of an Inconel 718 nickel alloy substrate test piece to enhance its resistance to surface wear and corrosion. The experimental procedure is shown in Fig. 1.

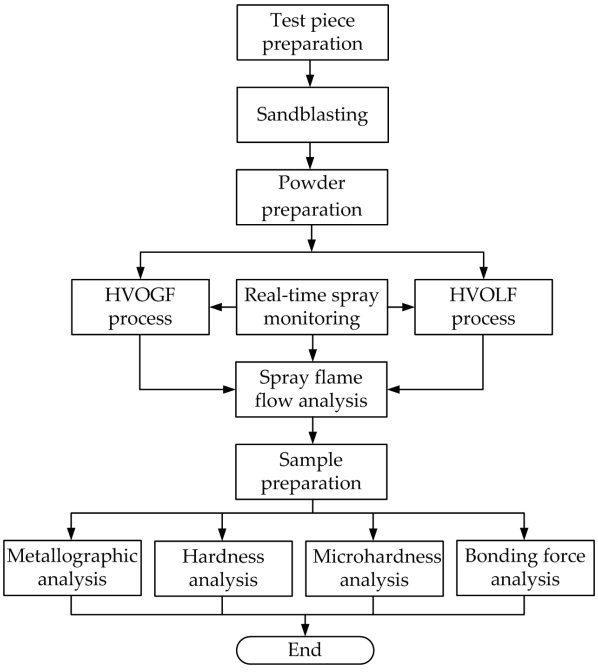

Fig. 1. Flowchart of the experimental procedure.

The chemical compositions of the cobalt-based Co–Mo–Cr–Si alloy powder (Co-111, Praxair Surface Technologies, Inc., USA) and Inconel 718 alloy substrate (UNS N07718) are presented in Tables 1 and 2, respectively.

2.1 Prepreparation

Before spraying, the surface of the test piece was wiped clean with acetone, and the boundary of the test surface was chamfered with a grinder to avoid the separation of the coating from the surface. After this initial cleaning, the piece was placed in an ultrasonic machine with acetone liquid for 10 min to fully remove contaminants and improve the physical bonding force between the coating and the substrate. Next, the piece was placed on the turntable of a siphon-type automatic sand-blowing machine (KS-110A, Qitian Co., Taiwan) and sandblasted with white alumina sand material #46 to roughen its surface and improve the mechanical bonding strength between the coating and the substrate. Finally, the sandblasted test piece was treated with dry high-pressure air to remove residual sand and dust from the surface. The size of the metallographic test piece used for metallographic analysis and surface hardness and microhardness tests was 38 × 19 × 1.6 mm^3. A 25.4-mm-diameter bonding force test stick was used for bonding force measurement.

2.2 Spraying and real-time monitoring system

To evaluate the effects that the two heat sources used in the high-speed flame spraying system had on the microstructural and mechanical properties of the coating, a diamond jet HVOGF spray gun (DJ-2700, Oerlikon Metco Co., Switzerland) and an HVOLF spray gun (WokaStar-610, Oerlikon Metco Co., Switzerland) were used in the experiments. During spraying, the test piece was placed on the turntable and rotated, and the spray gun was repeatedly moved from top to bottom by a computer-controlled system to completely spray the surface of the test piece until the desired thickness of 0.3–0.35 mm was reached, as shown in Fig. 2. The heat source in the HVOGF process used hydrogen and oxygen, and that in the HVOLF process used oxygen and aviation kerosene (JP-8). Table 3 shows the control parameters for the HVOGF and HVOLF spraying processes.

Table 1
Chemical composition of Co-111 powder.

Element	Mo	Cr	Si	Co
Wt (%)	27–30	16.5–18.5	3.0–3.8	Remainder
Size		<10 μm		

Table 2
Chemical composition of Inconel 718 alloy.

Element		C	Mn	Si	P	S	Cr	Ni	Mo	Nb +Ta	Ti	Al	Co	B	Cu	Fe
Wt (%)	Min.	—	—	—	—	—	17.0	50.0	2.80	4.75	0.35	0.20	—	—	—	Remainder
	Max.	0.09	0.35	0.35	0.015	21.0	21.0	55.0	3.30	5.50	1.15	0.80	1.0	0.006	0.30	—

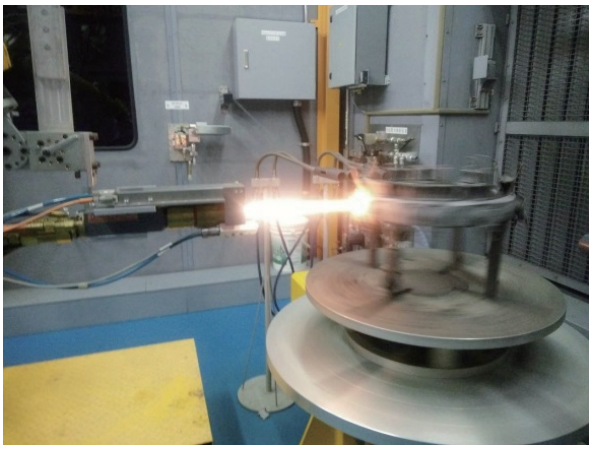

Fig. 2. (Color online) Test piece being sprayed using HVOGF or HVOLF.

Table 3
Parameters for high-velocity flame thermal spraying processes.

Parameters	HVOGF	HVOLF
Gun type	DJ-2700	Waka-610-Sz
O_2 flow rate (liter/min)	228.24	840.17
Fuel flow rate (liter/min)	742.15	2.43
Carrier gas (Ar) flow rate (liter/min)	13.30	9.34
Powder feed rate (g/min)	30	34
Spray distance (mm)	254	279.4
Gun speed (mm)	5.5	7
Turntable speed (RPM)	65	80
Preheating temperature (°C)	100	100
Coating thickness (mm)	0.35	0.35
Standard cubic feet per hour (SCFH)		

A real-time monitoring system was used to observe the flame characteristics of the HVOGF and HVOLF spray guns during spraying, specifically, the speed and intensity of the molten powder, the torch temperature, and the torch energy. Figure 3 presents a screenshot of the monitoring system, where A denotes the spray gun, B is where molten particle velocity and temperature were measured, C is the working line for measuring particle intensity, D is the particle spray centerline for measuring the distance from the gun to the test piece, E shows the particle intensity, F the particle velocity, G the molten particle temperature, and H the environmental temperature outside the test piece.

2.3 Postprocessing and measurement

After spraying, each test piece was subjected to cutting, hot mounting, grinding, and polishing to complete the metallographic preparation of the specimen. Cutting was performed to obtain the area required for metallographic observation. Cuts were directed into the coated surface to prevent the coating from peeling off. The main purpose of mounting was to make the observation surface parallel to the surface of the embedded test piece. The integrity of the

Fig. 3. (Color online) Real-time monitoring system for spray flame flow.

coating had to be preserved during grinding and polishing to ensure the correct measurement of the thickness and convenient observation for metallographic analysis.

A metallographic microscope and an image analyzer (Axioskop 2 Plus, Carl Zeiss Microscopy, LLC, United States) were applied to observe the cross section of the coating and the distribution of unmelted particles, and to calculate the porosity of the coating. The surface hardness of the coating was measured using a surface hardness machine (ATK-F3000, Mitutiyo America Corporation, USA) with a Rockwell 15N diamond indenter. Micro–Vickers hardness test equipment (HM-122, Akashi, Ltd.) was used to analyze the microhardness in accordance with the ASTM E384 standard specification.[20] The measurement of the bond strength between the thermal spray coating and the substrate was based on the method specified in ASTM C633.[21] After spraying, the bonding force test stick was glued to another loading rod using FM1000 epoxy adhesive and then placed in an oven for gluing treatment at 200 °C for 2 h. Figure 4 shows the measurement of the bonding strength of the coating at the substrate rod using a servo-controlled tensile testing machine (HT-2402, Hung Ta Co., Ltd., Taiwan).

3. Experimental Results and Discussion

3.1 Spray flame flow analysis

Table 4 presents the flame flow measurement data collected during the HVOGF and HVOLF spraying processes, specifically, particle velocity, plume temperature, and total intensity, where std stands for standard deviation. Notably, the HVOLF spraying process produced particles with 1.23 times higher velocity than by the HVOGF spraying process [1123.09 m/s (std 15.39) compared with 916.75 m/s (std 7.43)]. The plume temperatures of these two processes were very close and exceeded 2000 °C, which is enough to melt most thermal spray materials. Note also that the total intensity of the HVOLF spraying process was 1.33 times that of the HVOGF spraying process. Here, the arbitrary unit (arb. unit) is a relative unit of measurement to show the ratio of the intensity to a predetermined reference measurement. Therefore, it is important to compare the multiple measurements performed in similar environments.

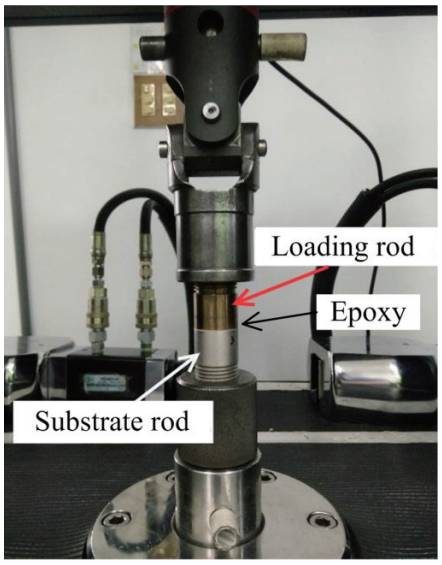

Fig. 4. (Color online) Setup of coating bond force test.

Table 4
Flame flow analysis data.

Method	Particle velocity (m/s)		Plume temperature (°C)		Total intensity (arb. unit)	
	Mean	Std	Mean	Std	Mean	Std
HVOGF	916.75	7.43	2086.28	7.50	30.46	0.70
HVOLF	1123.09	15.39	2142.62	3.84	44.1	0.185

3.2 Metallographic analysis

Figure 5 presents images of the metallographic structure of the coating in a cross section at 200× and 500× magnifications, obtained using an optical microscope. Unmelted particles (resembling balloons) are those in which the spherical or width-to-height ratio in the metallographic structure is less than 3:2, indicating that they were not flattened during the process. The observation of the metallographic structure at 200× using an optical microscope revealed an average of 3.7 and 0.6 unmelted particles in the cases of HVOGF and HVOLF, respectively, for 10 samples. The HVOLF spraying process clearly achieved excellent results. This is because the powder sprayed using this process had a high velocity and a large kinetic energy on impact, so the heated powder particles were more likely to be deformed and stretched flat on the surface of the substrate in a molten or semimolten state.

Before and after the deposition of droplets during spraying, the greater number of unmelted particles in the metallographic structure caused the unmelted particles to become stacked on each other, resulting in the formation of pores. Note that these pores were inside the coating and contained no substances. The molten particles and pores were proportional to each other; when the powder particles were more completely melted, the porosity of the coating was lower, and *vice versa*. In this experiment, the porosity of the coating was analyzed using an optical microscope and calculated using automatic image processing software. The average porosities

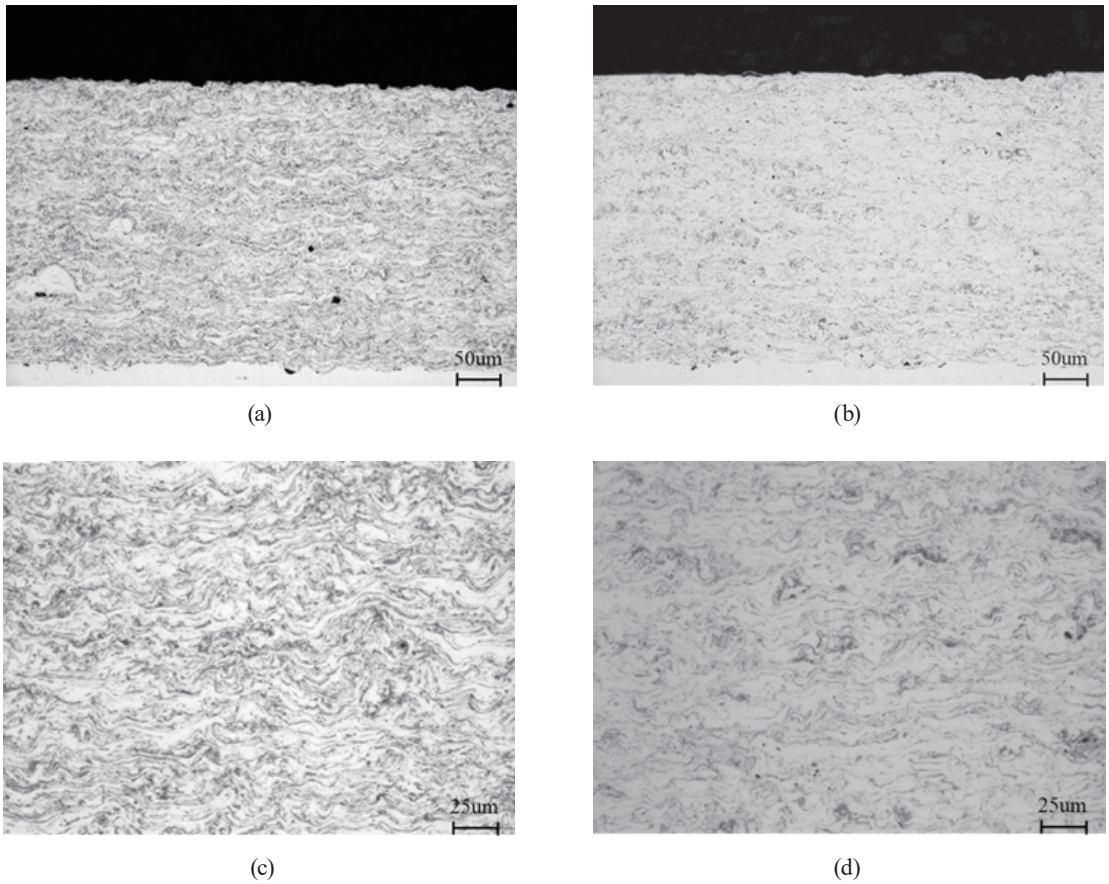

Fig. 5. Metallographic structure of the coating: (a) 200×, HVOGF; (b) 200×, HVOLF; (c) 500×, HVOGF; and (d) 500×, HVOLF.

of the metallographic structures resulting from the HVOGF and HVOLF spraying processes were 1.5 and 0.5%, respectively. According to the results of flame flow analysis, a higher particle velocity was achieved with HVOLF, so the resulting unmelted particles and porosity in the coated metallographic structure were inferior to those achieved with HVOGF. Figures 5(c) and 5(d) show 500× magnification images of the cross sections of the coatings sprayed with HVOGF and HVOLF, respectively. The layered structure of the cobalt-based coating is clearly visible. The spherical unmelted particles, pores, and oxides (dark gray) between the layers resulting from spraying with HVOGF are easily seen in the images of the metallographic structure.

3.3 Surface hardness and microhardness analyses

Surface hardness is defined as the resistance of a coating surface to indentation. It is a comprehensive index of the mechanical properties of a material, such as elasticity, plasticity, strength, and toughness. The higher the hardness, the higher the wear resistance. In experiments, the surface hardness test was carried out at 10 different places on each test piece.

The average surface hardnesses (R15N) for coatings formed by the HVOGF and HVOLF spraying processes are presented in Fig. 6. Note that the results were very close. However, the hardness of a coating is generally referred to as microhardness, which depends on the integrity and mechanical properties of the coating and has a significant impact on the wear resistance and strength of the coating. Figure 7 shows the average microhardness analysis results for 10 test pieces sprayed using HVOGF or HVOLF, measured with micro-Vickers hardness test equipment. It can be seen that the microhardness differs significantly, with that resulting from spraying with HVOLF being about 1.2 times that in the case of spraying with HVOGF. This is because the porosity and microhardness of a thermally sprayed coating are inversely related. When porosity is larger, the metallographic structure is looser and the measured microhardness is smaller. According to the results of metallographic analysis described in Sect. 3.2, the porosity obtained using the HVOLF spraying process was small, 0.5% compared with 1.5% obtained using the HVOGF spraying process. We therefore conclude that cobalt-based coatings sprayed with HVOLF have higher microhardness and superior wear resistance.

3.4 Bonding force analysis

In the bonding force experiment, we found that the fractured sections of the coatings sprayed with HVOGF and HVOLF were flat and exhibited no local cracking, as shown in Fig. 8. Figures 9 and 10 respectively depict the average bonding force and the stress–strain curves obtained by the bonding force test for the coatings formed by the two spraying processes. The average bonding forces obtained using the HVOGF and HVOLF spraying processes were, respectively, 25.04 and 41.43 MPa. That is, the average bonding force in the case of using the HVOLF spraying process was about 1.65 times that achieved when using the HVOGF spraying process. The HVOLF cobalt-based coating had a higher bonding force because the speed of the molten powder was higher than that obtained when using the HVOGF spraying process, so the corresponding kinetic energy on impact was larger. The metallographic structure was denser

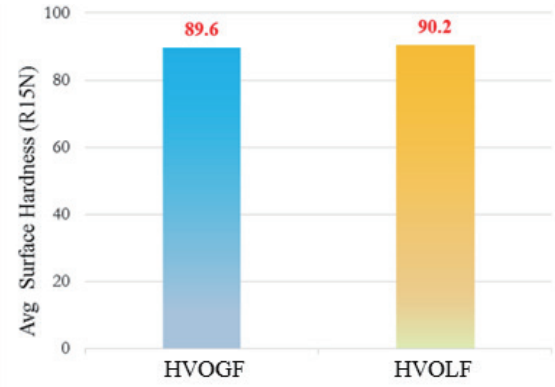

Fig. 6. (Color online) Surface hardness analysis results for HVOGF and HVOLF spraying processes.

Fig. 7. (Color online) Microhardness analysis results for HVOGF and HVOLF spraying processes.

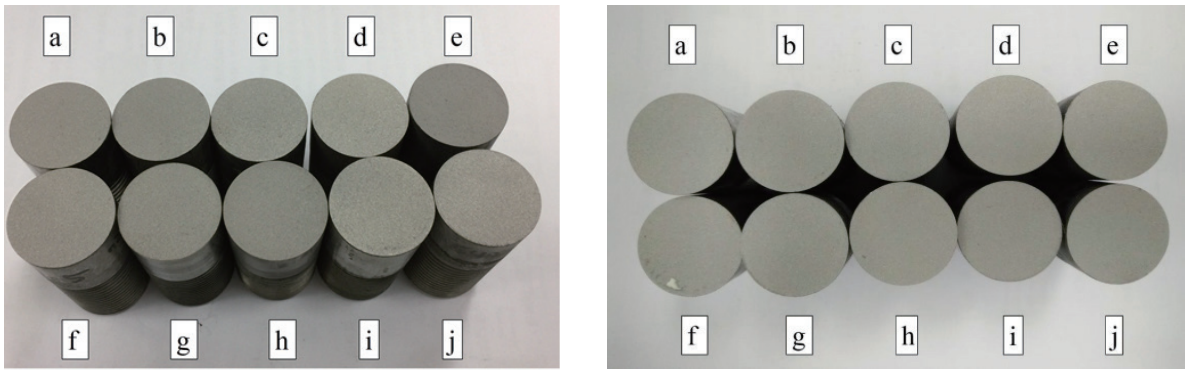

(a) (b)

Fig. 8. Test bars after bonding force test: (a) HVOGF and (b) HVOLF spraying processes.

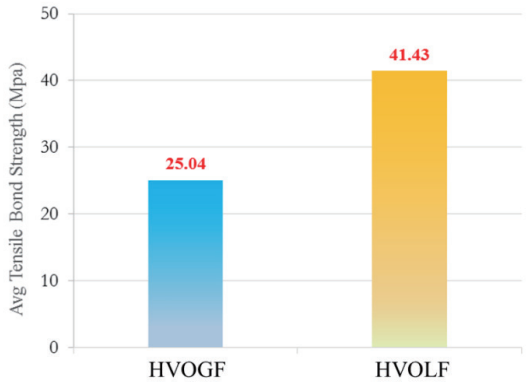

Fig. 9. (Color online) Average bonding force of the coating.

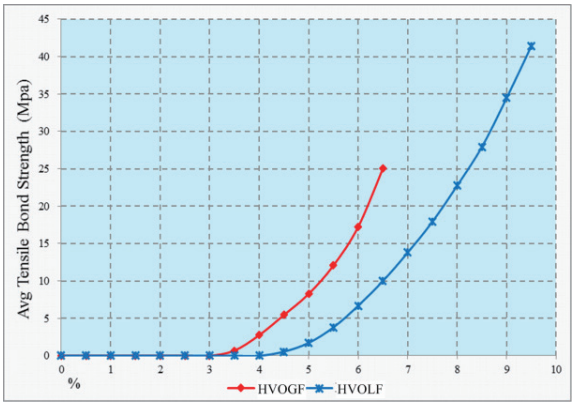

Fig. 10. (Color online) Stress–strain curve in the bonding force test.

when the velocity of the molten powder was higher, increasing the bonding force strength of the coating. In addition, as shown in Fig. 10, the test bar sprayed using HVOGF began to exhibit strain behavior at about 3.5%, but that sprayed using HVOLF did not show strain behavior until about 4.5% owing to the bonding force of the FM1000 epoxy adhesive between the loading rods and substrate rods.

4. Conclusions

In this study, HVOLF and HVOGF spraying processes were successfully used to coat a commercial powder of cobalt-based alloy onto the surface of an Inconel 718 nickel alloy substrate test piece. A real-time monitoring system enabled the observation of the torch temperature as well as the speed and strength of the molten powder during spraying. A comparison of the experimental results showed that powder particles sprayed with HVOLF flew 1.23 times faster and had 1.33 times greater intensity than those sprayed with HVOGF. However, the torch temperatures produced using these two heat sources were very close

and exceeded 2000 °C. According to the flame flow results, the HVOLF cobalt-based alloy powder had higher velocity and kinetic energy on impact, so the heated powder particles were more likely to be deformed and flattened on the surface of the substrate when in a molten or semimolten state. Hence, in the coated metallographic structure, the average number of unmelted particles and porosity arising from the HVOLF spraying process were, respectively, 0.6 and 0.5% within the test area. These values are smaller than those obtained when using the HVOGF spraying process. There was no significant difference in surface hardness between the processes. However, with respect to microhardness, the cobalt-based coating sprayed with HVOLF had a relatively high microhardness, and its average value was about 1.20 times that of the HVOGF coating because the porosity of the former was lower. Since the powder particles sprayed with HVOLF flew faster, the corresponding impact energy was higher, resulting in a denser metallographic structure and a coating bonding force of 41.43 MPa, which was 1.65 times the value obtained in the case of HVOGF.

The above-described results indicate that the cobalt-based alloy commercial powder sprayed with HVOLF onto the surface of an Inconel 718 nickel alloy substrate has superior mechanical properties to that sprayed with HVOGF under the same conditions. In the future, we will examine the thermal and structural properties of titanium alloy or ceramic coatings on turbine blades to enhance their resistance to wear, corrosion, and high-temperature oxidation.

Acknowledgments

This study was carried out at the Aerospace Industrial Development Corporation (AIDC). The authors are grateful for the equipment provided by AIDC and the partial financial support under grants MOST 106-2221-E-151-017 and MOST 106-2622-E-110-009-CC2.

References

1 A. M. Korsunsky, A. R. Torosyan, and K. Kim: Thin Solid Films **516** (2008) 5690.
2 R. J. M. Hague and P. E. Reeves: Rapid Prototyping, Tooling and Manufacturing (Rapra Technology Ltd., Wolverhampton, 2000).
3 N. P. Padture, M. Gell, and E. H. Jordan: Science **296** (2002) 280.
4 O. Metco: ipcm Protective Coatings **15** (2015) 48.
5 L. Pawlowski: The Science and Engineering of Thermal Spray Coatings (Wiley, New York, 2008).
6 K. H. Stern: Metallurgical and Ceramic Protective Coatings (Chapman & Hall, London, 1996).
7 R. C. Tucker: ASM Handbook, Volume 5A: Thermal Spray Technology (ASM International, Geauga, 2013).
8 J. M. Guilemany, J. M. Miguel, S. Vizcaino, and F. Climent: Surf. Coat. Technol. **140** (2001) 141.
9 P. Fauchais and A. Vardelle: Advanced Plasma Spray Applications (Intech Open Access Publisher, Rijeka, 2012) p. 1. https://doi.org/10.5772/34448
10 X. Ding, D. Ke, C. Yuan, Z. Ding, and X. Cheng: Coatings **8** (2018) 307. https://doi.org/10.3390/coatings8090307
11 N. D. Prasanna, C. Siddaraju, G. Shetty, M. R. Ramesh, and M. Reddy: Materials Today: Proc. **5** (2018) 3130.
12 S. Li, X. Yang, H. Qi, G. Xu, and D. Shi: Mater. Sci. Eng. A **678** (2016) 57.
13 A. Agüero, F. Camón, G. D. Blas, J. C. Hoyo, R. Muelas, A. Santaballa, S. Ulargui, and P. Vallés: J. Therm. Spray Technol. **20** (2011) 1292.
14 P. Vuoristo: Comprehensive Materials Processing, Volume 4: Coatings and Films: Thermal Spray Coating Processes (Elsevier Ltd., Amsterdam, 2014) p. 229. https://doi.org/10.1016/B978-0-08-096532-1.00407-6
15 N. Espallargas: Future Development of Thermal Spray Coating: Introduction to Thermal Spray Coatings (Elsevier Ltd., Amsterdam, 2015) p. 1.

16 V. Kumar and B. Kandasubramanian: Particuology **27** (2016) 1.
17 B. Song, Z. Pala, K. T. Voisey, and T. Hussain: Surf. Coat. Technol. **318** (2017) 224.
18 T. Fiedler, H.-R. Sinning, J. Rösler, and M. Bäker: Surf. Coat. Technol. **319** (2018) 32.
19 P. Puddu, S. Popa, G. Bolelli, P. Krieg, M. L. Gualtieri, L. Lusvarghi, A. Killinger, and R. Gadow: Surf. Coat. Technol. **319** (2018) 677.
20 ASTM E384. Standard test method for microhardness of materials (ASTM International, West Conshohocken, 2013).
21 ASTM C633. Standard test method for adhesion or cohesion strength of thermal spray coatings (ASTM International, West Conshohocken, 2013).